A Study of a Mesoscale Solitary Wave in the Atmosphere Originating near a Region of Deep Convection

YUH-LANG LIN*

Department of Physics and Atmospheric Science, Drexel University, Philadelphia, Pennsylvania

R. CRAIG GOFF**

National Severe Storms Laboratory, Norman, Oklahoma

(Manuscript received 30 June 1986, in final form 28 July 1987)

ABSTRACT

An analysis of a mesoscale wave which occurred over the eastern United States on 6 March 1969 is presented. Its origin is attributed to the perturbation of a midtropospheric inversion by a squall line. After the wave formed, it propagated in the direction of the mid- and upper-level tropospheric flow and expanded as an arc with the center located near the region of convective activity. The wave traveled from western Tennessee and Kentucky over a distance of more than 1000 kilometers to Nova Scotia with a mean speed of 55 m s^{-1}. The event was quite obvious on surface barographs throughout this region. Pressure traces showed an obvious V-shaped pressure drop of 3 to 6 mb over much of the wave path. The wave persisted for about 9 hours with little change in character.

The synoptic situation is analyzed and compared with similar atmospheric conditions in other studies. The generation mechanism of an internal gravity wave of depression is investigated by a simple model. It is found that waves of depression or elevation are described by a nondimensional number $M = Nz_1/\sqrt{g'H}$ which is related to the depth and strength of the inversion, the stratification above the inversion, and the position of the heat source. The effects of nonlinearity and dispersion are determined to be the same order of magnitude. A theory of Gear and Grimshaw is used to describe the basic character and to calculate the phase speed and wavelength of the solitary wave. The theoretical description corresponding to the lowest eigenvalue mode describes the basic character of the disturbance as a wave of depression with a preferred propagation in the direction of the basic flow. Both characteristics are verified by observation. The phase speed calculated by the theory compare favorably with the observed values.

1. Introduction

Propagating waves on order of 100 km are often observed in the atmosphere. Some waves tend to trigger, enhance or reorganize new or existing convective storms (Uccellini, 1975; Miller and Sanders, 1980; Stobie et al., 1983), while others may or may not be associated with deep convection, but may travel several hundred kilometers, and persist for considerable time with little change of their characteristics (Brunk, 1949; Wagner, 1962; Ferguson, 1967; Bosart and Cussen, 1973; Eom, 1975; Pecnick and Young, 1984; Bosart and Sanders, 1986). Waves of the latter type, being isolated quasi-steady disturbances of permanent form, may in some instances be manifestations of "solitary waves". These waves have been studied extensively in last two decades. Existing theories have been categorized as (e.g., see Koop and Butler, 1981): (a) shallow water theory: the classical KdV-type solitary wave (Benjamin, 1966), (b) deep-water theory: the algebraic solitary wave (Benjamin, 1967; Davis and Acrivos, 1967; Ono, 1975), and (c) finite-depth theory (Joseph, 1977).

Propagating atmospheric mesoscale solitary waves are usually revealed by surface pressure perturbations having wave amplitudes of a few millibars. Observations indicate that these waves may occur as internal solitary waves of elevation (Abdullah, 1955; Christie et al., 1978) or internal solitary waves of depression (Christie et al., 1978; Pecnick and Young, 1984). For a fixed upper boundary, internal solitary waves in the lowest mode are either waves of elevation or depression depending on the detailed fluid density and shear structure (Long, 1965; Benjamin, 1966; Miles, 1979; Maslowe and Redekopp, 1980; Gear and Grimshaw, 1983). Notice that the only eigenvalue mode of interest in the interpretation of atmospheric waves is the lowest mode since higher modes almost invariably propagate much slower than the lowest mode and are not generally observed in either geophysical environments or

* Present affiliation: Department of Marine, Earth, and Atmospheric Sciences, North Carolina State University, Raleigh, NC 27695.
** Federal Aviation Administration.

Corresponding author address: Mr. Craig Goff, Federal Aviation Administration, APS-550, 800 Independence Ave. SW, Washington, DC 20591.

in laboratory experiments. For a two-layer fluid system with no vertical shear, waves of depression or elevation are determined by the depth and density of each layer (Peters and Stoker, 1960). In several case studies of solitary waves, the layer above the inversion is observed to be only weakly stratified. Under these conditions, the wave can propagate horizontally for long periods of time since the energy loss due to radiative damping is small (Maslowe and Redekopp, 1980; Grimshaw, 1980/81, 1981a; Crook, 1986).

It is known that thunderstorm systems may serve as a source of internal gravity waves with wavelengths on the order of 10 km (Curry and Murty, 1974; Erickson and Whitney, 1973; Haase and Smith, 1984; Doviak and Ge, 1984), and internal gravity waves with wavelengths on the order of 100 km (Wagner, 1962; Ferguson, 1967; Bosart and Cussen, 1973).

In studying mesoscale gravity waves of isolated form, some authors (e.g., Wagner, 1962) have applied or modified linear theories of gravity waves to calculate the phase speeds. In some cases, phase speeds calculated by this type of model are close to the observed values. However, short internal dispersive gravity waves either tend to decay too rapidly, or occur as sinusoidal wavetrains, characteristics markedly different from the long lifetime mesoscale waves of isolated form. Further, Lindzen and Tung (1976) found that mesoscale linear gravity waves could be ducted if there exists a stable duct adjacent to the surface wherein the mean flow at some altitude either equals or comes close to the phase speed of the waves. However, those requirements for a stable duct are not often met by observed mesoscale waves of isolated form.

In this paper, we present an analysis of an isolated mesoscale wave of depression. The wave characteristics, origin, and synoptic situation are discussed and compared with similar observations. A simple model with a sharp inversion and a pulse heat source is solved as an initial value problem to help understand the formation mechanism of waves of depression or elevation. The relative importance of nonlinearity and dispersion will be investigated. A second-order classical solitary wave theory developed by Gear and Grimshaw (1983) is used to describe the wave behavior and to calculate its phase speed and wavelength.

2. Synoptic situation

On the morning of 6 March 1969, a surface low pressure area just off the Louisiana coast was moving slowly eastward and intensifying. Associated with the surface low, a warm front extended eastward to the Florida coast and a cold front extended southward from the low pressure center into the Gulf of Mexico. The surface pattern had strong support from a deep upper level trough which was moving rapidly eastward from near 100°W longitude. Figure 1 shows the 1200 UTC position of the 500 mb trough and the high speed flow south and east of the trough.

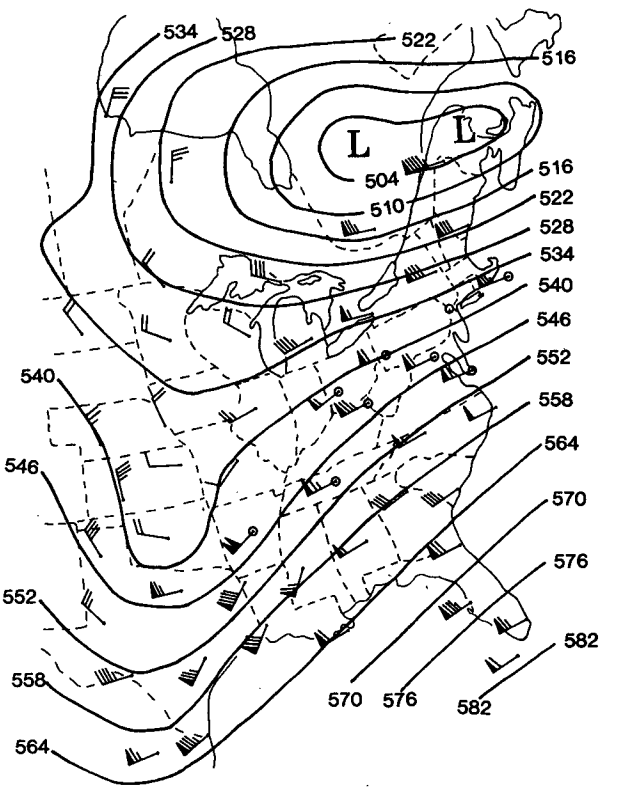

FIG. 1. 500 mb chart for 1200 UTC 6 March 1969. Heights in decameters. Small circles are stations for the profiles in Fig. 7.

A prefrontal squall line had developed in east Texas during the previous evening and moved eastward at about 15 m s^{-1}. By 1100 UTC it was located on a line from New Orleans to near Tupelo, Mississippi (Fig. 2a). A few hours earlier, a propagating surface mesolow was observed in the northern Alabama and Mississippi region near the north end of the squall line, and as the disturbance propagated toward the northeast, it was observed to elongate along an axis normal to its movement. The squall line continued to move southeastward (to the right of the mean flow) and dissipated, especially on the north flank, while the mesolow migrated toward the northeast. The meso-low moved in the same direction as the mid- and upper tropospheric flow (Fig. 1).

Figure 2a–c are surface pressure maps with contour positions determined by combining hourly surface observations and barograph traces using appropriate interpolation between stations where necessary. At a mean propagation speed of about 55 m s^{-1}, the mesolow quickly moved away from the prefrontal squall line region, and in a 4-hour period ending at 1500 UTC had moved nearly 800 km to central New York (Fig. 2c). The surface wind pattern at 1300 UTC 6 March 1969 relative to the convergence line associated with the solitary wave is illustrated in Fig. 3 just as the wave entered Pennsylvania (see Fig. 2b), about one hour after maximum amplitude of the mesolow. The axis of con-

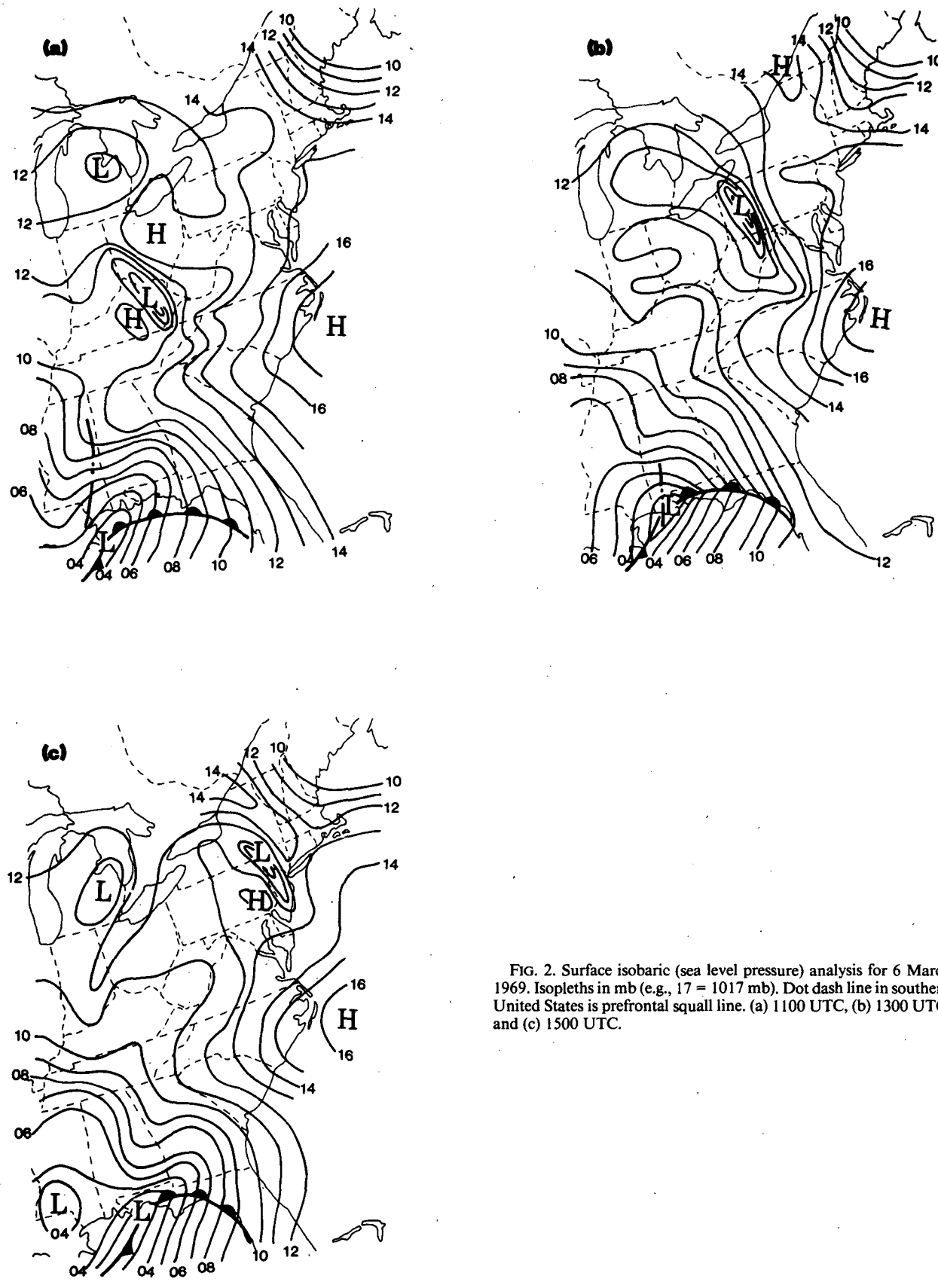

FIG. 2. Surface isobaric (sea level pressure) analysis for 6 March 1969. Isopleths in mb (e.g., 17 = 1017 mb). Dot dash line in southern United States is prefrontal squall line. (a) 1100 UTC, (b) 1300 UTC, and (c) 1500 UTC.

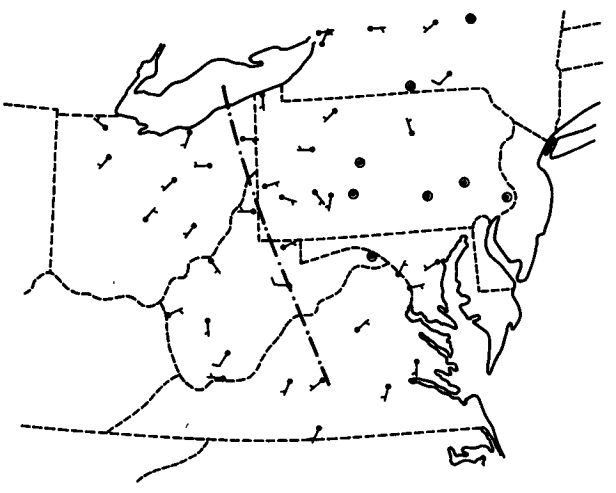

FIG. 3. Surface wind pattern at 1300 UTC 6 March 1969 and the surface convergence line (dot-dash line) associated with solitary wave. Full barb is 5 m s^{-1}.

vergence, denoted by the dot-dash line, is behind the trough line. Convergence values are generally larger than 10^{-4} s^{-1} within 25 km of the line.

3. Solitary wave detection and analysis

Evidence for a propagating mesoscale gravity wave of depression appears in numerous Atlantic coastal region barograph traces. Figure 4 shows the surface pressure disturbance observed at selected stations. Most of the barographs reveal a "V-shaped" pressure drop of 3 to 6 mb in an interval of about 2 hours. The amplitude of the pressure disturbance generally increases to a maximum at stations in central West Virginia and western Pennsylvania and, thereafter, decreases as the wave moves toward the Atlantic coast and Nova Scotia. An analysis of the pressure trace data indicates that the largest pressure perturbation is about 6 mb at Charleston, West Virginia (CRW) and Pittsburgh, Pennsylvania (PIT). Small positive pressure perturbations before and after the V-shape pressure drop are also noticeable. The disturbance is characterized by an elongated low center (Fig. 2) and a retention of its basic size and shape throughout its life. As will be shown, this propagating mesoscale trough line can be regarded as a manifestation of an internal solitary wave of depression.

Figure 5 depicts the hourly movement of the solitary wave. The wave originates near the region of strong convective activity in Alabama and Mississippi in the early morning of 6 March. It then propagates northeastward and expands within an arc of about 40° whose origin is located in central Mississippi. The disturbance is not a critical wave phenomenon since at no altitude does the wave phase speed equal the wind component in the direction of wave propagation. The average speed of the wave is about 55 m s^{-1} during its observed lifetime. Undulations in the isochrones in Fig. 5 may be due more to time errors in the station barograph charts than variations in the speed of the wave.

Near the wave's origin, the southern Appalachian Mountains, the lower troposphere is quite moist, as shown in Fig. 6. As the wave trough intensifies and moves away from the convective zone in Alabama and Mississippi, the forward edge of a light precipitation band moves northward nearly coincident with the wave front. There is no evidence of deep convection with this precipitation band. Table 1, which gives the precipitation onset time and time of lowest pressure at five stations in the wave path, indicates that the wave trough precedes the onset of precipitation at each station by 5 to 20 min. This is consistent with the observation in Fig. 3 that the trough line precedes a line of maximum surface convergence. The line of maximum surface convergence following the trough line is a manifestation of a circulation couplet associated with the wave. Maximum subsidence occurs along the trough line with the tendency for positive vertical motion on either side. However, the circulation in the part of the couplet in advance of the trough is suppressed by the effects of the wave propagation and enhanced in the part of the couplet behind the trough. The result

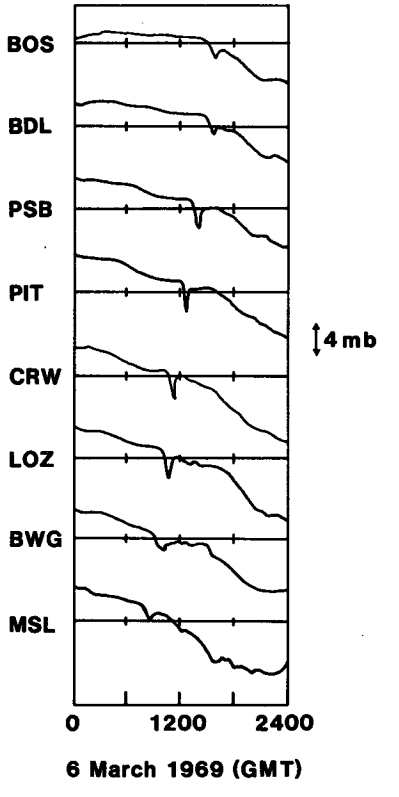

FIG. 4. Surface pressure traces for select stations on 6 March 1969: (1) BOS—Boston, MA, (2) BDL—Hartford, CT, (3) PSB—Philipsburg, PA, (4) PIT—Pittsburgh, PA, (5) CRW—Charleston, WV, (6) LOZ—London, KY, (7) BWG—Bowling Green, KY, (8) MSL—Muscle Shoals, AL.

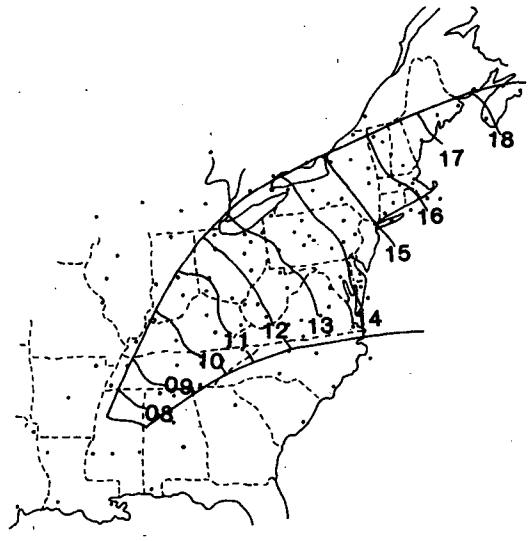

FIG. 5. Solitary wave hourly isochrones and wave boundaries. The numerical values refer to trough passage time (hour UTC) of the wave.

is much greater positive vertical motion behind the trough than in advance of the trough. This trough line precursor is about one quarter the wave period (defined as the time between the ridge peaks before and after the trough ~1 h) and develops a situation in which the low-level ambient flow relative to the wave is from the front to the back of the wave. In the drier atmosphere northeast of Louisville, Kentucky (SDF) the onset of rain no longer tracks with the trough.

Table 2 lists the cloud chronology at five eastern U.S. stations. The time that the solitary wave trough

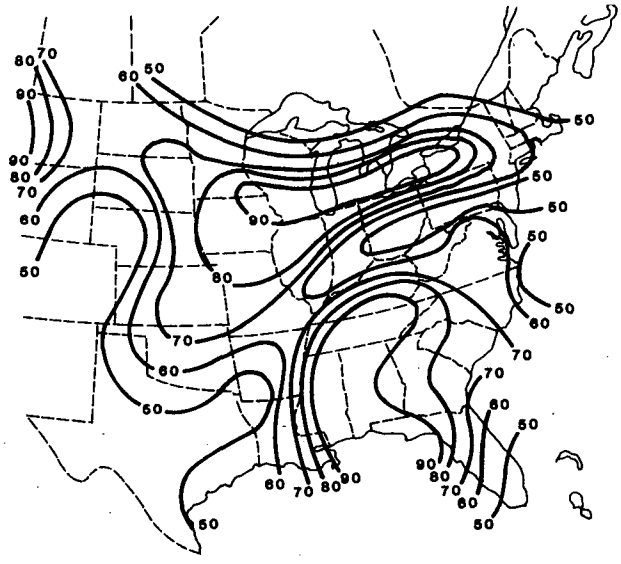

FIG. 6. Relative humidity averaged from the surface to 500 mb at 1200 UTC 6 March 1969.

TABLE 1. Chronology at five southeastern U.S. stations[a] 6 March 1969 (Times are UTC)

	MSL	HSV	CSV	SDF	LEX
Precipitation began	0812	0848	0945	1057	1055
Trough passage	0800	0842	0930	1037	1050

[a] MSL = Muscle Shoals, AL; HSV = Huntsville, AL; CSV = Crossville, TN; SDF = Louisville, KY; LEX = Lexington, KY.

was observed at each station is shown in parentheses. Observations at Elkins, West Virginia (EKN) and Harrisburg, Pennsylvania (HAR), indicate that low clouds were only observed close to trough passage time. At all other stations except Parkersburg, West Virginia (PKB), the mesolow passage coincided with the onset of middle level clouds which indicates that the disturbance has considerable vertical extent.

Upper air station spacing does not allow entirely adequate detail of the wave but some interesting observations can be made from the available data. Figure 7 illustrates nine temperature soundings made at 1200 UTC. The soundings are spaced along the 500 mb line, the arbitrary abscissa. The spacing is proportional to real distances between station positions projected onto an imaginary 543 dm line (Fig. 1). All profiles show a midtropospheric inversion of varying thickness, intensity, and location in the 480 to 630 mb layer. This inversion is considered to be the propagation medium of the wave. First, it is assumed that the inversion centered near 510 mb at BNA and about 50 to 75 mb lower at PIT and DCA is continuous at intermediate locations along this swath. Then it is claimed that this is the same inversion which is depressed to about the 750 to 780 mb level at DAY and HTS. If in fact the continuity assumption is valid, then the potential temperature contours in Fig. 8 bear out the observation that the effect of the wave appears to dramatically influence both the DAY and HTS soundings in Fig. 7. These soundings were taken at approximately the time the wave passed over these stations. Note that soundings are typically released 45 minutes prior to the stated observation time. Extending the continuity assumption to include the inversion centered near 500 mb at LIT, WAL, TEB, and ACK (Nantucket, Massachusetts), it is thereby claimed that this midtropospheric inversion and the lower stable layer provides a base for the solitary wave to form and to propagate horizontally for long distances.

Potential temperature data shown in Fig. 8 have been interpolated, then filtered by a 9-point filter (e.g., see Haltiner and Williams, 1980). The figure shows a large amplitude potential temperature waveform in the DAY/HTS area, a manifestation of the solitary wave. The disturbance can be recognized throughout the troposphere but is not a significant feature above the tropopause. The average oscillation amplitude is roughly

TABLE 2. Cloud chronology at five eastern U.S. stations[a] (Times are UTC).

Trough time	PKB (1205)	EKN (1259)	PSB (1340)	HAR (1355)	ABE (1440)
1100	U⊕	/-◐	U◐	/-◑	/-◐
1200	E60◐/⊕	80◐U⊕	U◐	150-◐/-⊕	/-◐
1300	E60⊕	30◑E120◐/⊕	U⊕	150◑/-⊕	/-◐
1400	60◑E100⊕	120◑U⊕	E120◐/⊕	80◑E120⊕	/-◐
1500	E60⊕	120◑U⊕	E100◐/⊕	E120⊕	E120◐/⊕

[a] PSB = Philipsburg, PA; ABE = Allentown, PA. Cloud cover symbols are defined as (1) ○—clear (<0.1), (2) ◑—scattered (0.1–0.6), (3) ◐—broken (0.6–0.9), and (4) ⊕—overcast (>0.9). Other station codes are given in the text.

75 mb. Weak high pressure ridges in the surface traces ahead of and behind the trough (Fig. 4) are also evident in the potential temperature field. Near Wallops Island, there exists another weak wave of depression, which might be a second internal solitary wave, the dispersive tail associated with the inbalance of nonlinearity and dispersion, or the manifestation of baroclinicity as Wallops Island is on the warm side of the imaginary 543 dm line (see Fig. 1).

The analyzed Brunt–Väisälä frequency for DAY (1200 UTC) is plotted in Fig. 9. Comparing the observations in Fig. 7 with those of Fig. 9, we see that above the midtropospheric inversion observed in Fig. 7, there exists a weakly stratified layer. A weakly stratified upper layer above the inversion waveguide is an important requirement for internal solitary wave propagation since under these conditions the energy loss due to radiative damping is small (Maslowe and Redekopp, 1980; Grimshaw, 1980/81, 1981). The dissipation of the solitary wave downstream is partly due to the radiation damping of this upper tropospheric layer and wave spread in the lateral direction. The wind direction is quite uniform in the vertical except in the very low layer where boundary effects are influential. The wind speed increases upward to a maximum value of about 60 m s^{-1} at 300 mb.

4. Origin of the internal wave of depression

Figure 5 indicates that the wave described can be traced back to a region of strong convective activity in Alabama and Mississippi in the early morning of 6

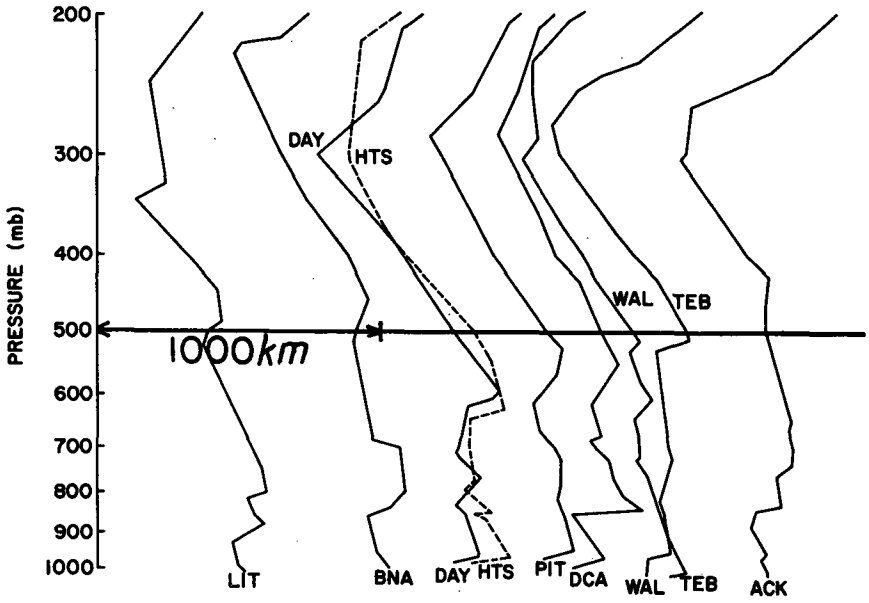

FIG. 7. Temperature profiles at 1200 UTC, 6 March 1969 for nine stations projected to a surface intersecting the 543 dm height inferred in Fig. 1. Stations are scaled along the 500 mb line, not the surface. Profiles show the midtropospheric inversion (450 mb to 650 mb) upon which the wave described propagates. The diagram is a skew T-log p chart. (1) LIT: Little Rock, AR, (2) BNA: Nashville, TN, (3) DAY: Dayton, OH, (4) HTS: Huntington, WV, (5) PIT: Pittsburgh, PA, (6) DCA: Washington, DC, (7) WAL: Wallops Is., VA, (8) TEB: New York City (Teterboro Airport), (9) ACK: Nantucket, MA.

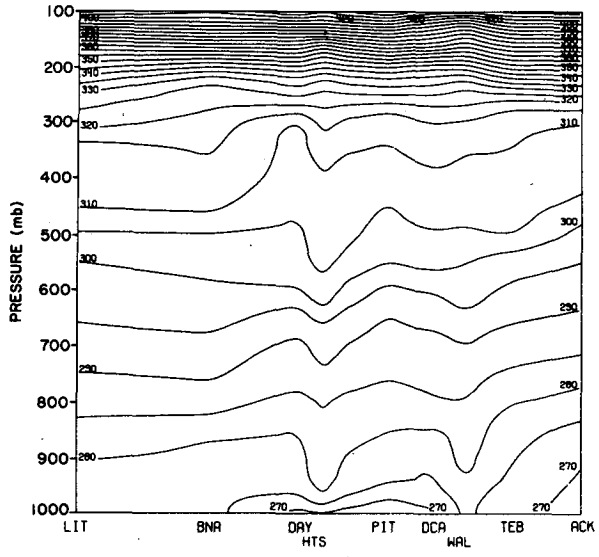

FIG. 8. Isentropic analysis (°K), using sounding data projected to an 543 dm height line, whose position is inferred in Fig. 1. See Fig. 7 for station identifiers.

March. There are numerous reports in the literature which claim that strong convection may generate waves that propagate away from a thunderstorm area (e.g., Wagner, 1962; Ferguson, 1967; Bosart and Cussen, 1973). When the phase speed of such a wave is high, the implication is that the disturbance is associated with the higher altitude atmospheric structure (Christie et al., 1978), and in our case, the data suggest that the wave is a manifestation of a disturbance on the mid-tropospheric inversion and within the deep stable layer. In several studies of mesoscale waves (e.g., Ferguson, 1967) it was found that deep convection had disturbed the midtropospheric inversion. In the 6 March case, the wave generation may be due to the forming by deep convection.

The generation mechanism of an internal wave of depression by a thunderstorm is described by a model developed by Smith and Lin (1982) and Lin and Smith (1986) which has been modified to include: 1) a sharp temperature inversion, 2) a zero basic wind, and 3) a variation of buoyancy frequency. The model assumes a two-dimensional, inviscid, non-rotating, hydrostatic, low Mach number flow. The small amplitude equation for the vertical velocity is written as

$$w_{ttzz} + N^2(z)w_{xx} = (g/c_p\bar{T})q_{xx}, \qquad (1)$$

where $N(z)$ is the buoyancy frequency, $\bar{T}$ is the basic state temperature, and q is a heating rate per unit mass. For simplicity, we consider a simple case with

$$N(z) = N[\delta(z) + S(z)], \quad -H < z \qquad (2)$$

$$q(t, x, z) = Q_0\delta(t)[b^2/(x^2 + b^2)]\delta(z - z_1), \; z_1 > 0, \qquad (3)$$

where δ is a Dirac delta function, S is a step function, Q_0 is the amplitude of the heating, and b is the half-width of the heat source. The units of Q_0 are J kg^{-1} s^{-1}. Note that the origin of z is elevated above the ground. In Eq. (2) we assume a delta function of the buoyancy frequency at $z = 0$, which represents a sharp temperature inversion riding on a neutrally stratified layer of depth H. The buoyancy frequency (N) is constant in the upper layer above the inversion. The heat source is released instantly as a pulse and concentrated at $z = z_1$ [Eq. (3)]. The diabatic heating expressed in Eq. (1) is assumed to be a diabatic mass flux generated by cumulus development (Raymond, 1983).

The problem is solved by determining the relevant Green's function. Taking Fourier transforms in t and x of (1) and (3) gives

$$\hat{w}_{zz} + (Nk/\omega)^2\hat{w} = [gQ_0bk^2\exp(-b|k|)/(4\pi c_p\bar{T}\omega^2)]\delta(z - z_1). \qquad (4)$$

The lower boundary condition is $\hat{w} = 0$ at $z = -H$, while the appropriate upper boundary condition is the radiation condition, i.e., $\hat{w} \sim \exp(iN|k|/\omega)$ as $z \to \infty$. There are four interface conditions. At the interface $z = z_1$, $\hat{w}$ is continuous across the interface. Integrating Eq. (4) across the interface yields another condition that $\hat{w}_z$ is continuous. Likewise, at the inversion $z = 0$, $\hat{w}$ is continuous across the inversion and integrating Eq. (4) across $z = 0$ yields a condition which relates to the strength of the inversion; that is, $g' = g\Delta\theta/\bar{\theta}$ (Geisler

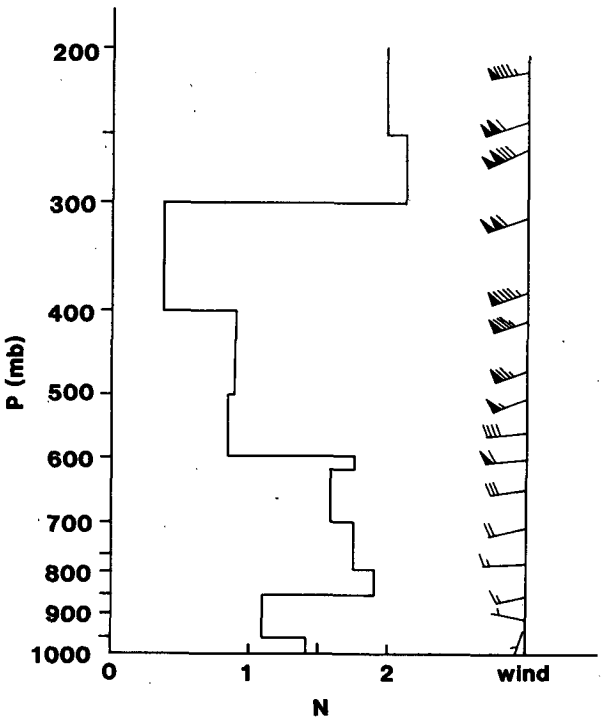

FIG. 9. The Brunt-Väisälä frequency and DAY wind profile at 1200 UTC 6 March 1969. The units of the Brunt-Väisälä frequency are 10^{-2} s^{-1}.

and Bretherton, 1969). The solution in the lower layer ($-H < z < 0$) is

$$\eta = \frac{igQ_0b(z+H)}{4\pi c_p\bar{T}}\int_{-\infty}^{\infty} k^2 e^{(-b|k|+ikx)}dk \times \int_{-\infty}^{\infty} \frac{e^{i(Nz_1|k|/\omega+\omega t)}}{\omega(\omega^2 - iNH\omega|k| - g'Hk^2)}d\omega, \quad (5)$$

where η is the vertical displacement and is defined as $\eta = \int w dt$. A closed form of (5) is possible but is lengthy. An asymptotic form is obtained by applying the method of stationary phase (appendix A) for large t and x

$$\eta = \frac{-gQ_0bt^2(z+H)\exp(-bNz_1t/x^2)}{2c_p\bar{T}|x|[(x^2 - g'Ht^2)^2 + (NHtx)^2]}\left[(x^2 - g'Ht^2) \times \sin\left(\frac{Nz_1t}{|x|}\right) + NHt|x|\cos\left(\frac{Nz_1t}{|x|}\right)\right]. \quad (6)$$

We now introduce nondimensional variables by scaling x by b, z and η by H, t by b/c_0, and Q_0 by $c_p\bar{T}c_0^2/g$. Equation (6) then becomes

$$\eta = \frac{-(z+1)Q_0t^2\exp(-Mt/x^2)[(x^2 - t^2) \times \sin(Mt/|x|) + Ftx\cos(Mt/|x|)]}{2|x|[(x^2 - t^2)^2 + (Ftx)^2]}, \quad (7)$$

where c_0 is the linear internal shallow water phase speed, i.e., $\sqrt{g'H}$, which is related to the strength of the inversion. The two nondimensional numbers M and F are defined as Nz_1/c_0 and NH/c_0, respectively. The parameter F represents a heating-induced Froude number defined by Lin and Smith (1986). The wave is considered a long wave because the width of the wave (185 km) is much larger than the depth of the lower layer.

A similar result can be obtained for a case of a neutrally stratified layer overriding a stable layer of depth H with no inversion in between. Instead of $\sqrt{g'H}$, the linear internal shallow water phase speed (c_0) becomes $2NH/\pi$ (e.g., see Case IIIA of Grimshaw, 1981b). Thus, the presence of an inversion plays the same role as the lower stable layer, that is, it provides a base for the wave to form and to travel horizontally.

To investigate the qualitative behavior of the disturbance on the midtropospheric inversion produced by latent heating associated with a squall line, we consider a case with the non-dimensional values $M = 0.1$, $F = 1.0$, and $Q_0 = 0.5$, and the dimensional values $H = 5500$ m, $z_1 = 550$ m, $c_0 = 55$ m s^{-1}, and $N = 0.01$ s^{-1}. The results of a calculation for the right-moving wave for four values of t are depicted in Fig. 10. A wave with negative displacement is produced by the latent heating, which then propagates away from the source region ($x = 0$). The propagating gravity wave is dispersive and decays gradually. If nonlinear effects are included and if the inversion waveguide structure supports the propagation of solitary waves of depression, a balance between the competing effects of steepening and frequency dispersion will occur as the initial long wave disturbance evolves asymptotically in time into one wave. These solitary waves of depression will then continue to propagate along the inversion, away from the source region, as isolated waves of permanent form. In contrast, if the ambient waveguide structure does not support solitary waves of depression, an initial long-wave perturbation of this type decays eventually only into a long oscillatory train of dispersive waves. In the present case, the available evidence indicates that an initial disturbance caused by latent heat production near a midtropospheric inversion has led to the formation of a single solitary wave of depression.

The generation mechanism considered here may also lead to favorable circumstances for the creation of solitary waves of elevation on a low altitude inversion. Figure 10 indicates that the wave of depression travels toward the right with a speed roughly equal to the shallow water wave speed c_0 which corresponds to the nondimensional wave speed 1. Following the wave trough by letting $x = t$ in Eq. (7), it can be shown that η changes sign at $M = \pi/2, 3\pi/2, \cdots$, etc. Thus the wave is a wave of depression or elevation depending upon the nondimensional number M which is determined by the heating location (z_1), stratification (N), the depth of the shallow layer (H), and the strength of the inversion (g'). This effect on M is caused by the cancellation of the downward directed energy flux of the wave and upward directed energy flux of the wave reflected from the ground.

A case with $M = 2.0$, $F = 1.0$ and the dimensional values $H = 1000$ m, $z_1 = 2000$ m, $c_0 = 10$ m s^{-1}, and $N = 0.01$ s^{-1} is depicted in Fig. 11. Differences in the scaling factor H significantly influence the amplitudes of the nondimensional vertical displacements (η) in Figs. 10 and 11. In Fig. 11, the wave generated at the inversion is a wave of elevation. It can be anticipated that an initial long wave disturbance of this type will evolve into a finite number of amplitude-ordered sol-

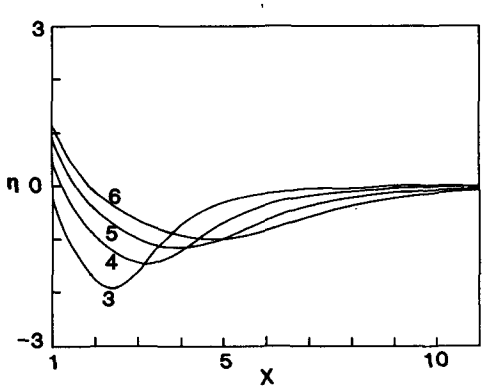

FIG. 10. The vertical displacement at the inversion level ($z = 0$) with $M = 0.1$, $F = 1$, and $Q_0 = 0.5$ for $t = 3, 4, 5, 6$. The formula is given in Eq. (7).

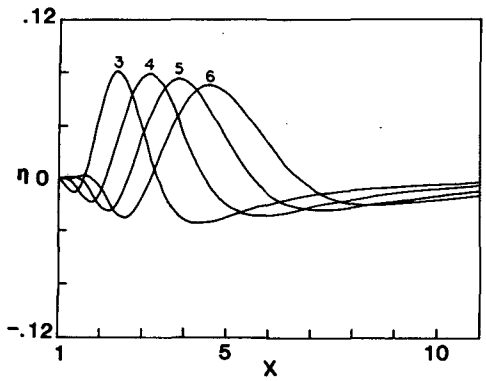

FIG. 11. As in Fig. 10 except $M = 2$ and $F = 1$. Notice the scale of η is different from that of Fig. 10.

itary waves of elevation followed by a relatively weak dispersive wave train. As can be seen from Fig. 11, weak negative vertical displacements exist on both sides of the initial long wave disturbance. These negative disturbances tend to decay relatively rapidly. It appears that a model of this type with $M = 2$ and $F = 1$ could provide an explanation for the observations reported by Wagner (1962) of long waves of elevation propagating on a lower altitude inversion layer.

5. Verification of the solitary wave

Existing theories of internal solitary waves have been categorized by Koop and Butler (1981). They are summarized here for the purposes of verifying that the observed wave is indeed a solitary wave, and determining the appropriate theory for the observed wave. There are three theories applied to internal solitary waves:

(i) shallow water theory for the classical KdV-type solitary wave (Benjamin, 1966)

$$L/h \gg 1, \quad d/h = \mathrm{O}(1);$$

(ii) deep-fluid solitary wave (Benjamin, 1967; Ono, 1967; Davis and Acrivos, 1967)

$$L/h \to 0, \quad L/d \gg 1;$$

(iii) finite-depth theory (Joseph, 1977)

$$L/d \gg 1, \quad d/h \ll 1.$$

For these theories, L is the horizontal scale of the wave, h is the total fluid depth, and d is an intrinsic vertical length scale associated with the density stratification. For the present case, one might choose L as the width of the wave (~185 km), d as the depth of the lower stable layer (~5000 m) and h as the total depth of the troposphere (~9000 m) since there is an abrupt increase of the stability at the tropopause (Fig. 9). Thus the ratio L/h is about 20.5 or much larger than 1. The ratio d/h is about 0.55. This suggests that this wave falls into the category of classical KdV-type solitary waves. Thus, this wave is different from the morning glory wave which is considered to be a deep-fluid solitary wave (Christie, et al. 1979; 1981). The finite-depth theory of solitary waves is not appropriate for the internal solitary wave as described herein, because the magnitude of d/h is close to order 1.

Gear and Grimshaw (1983) propose a solitary wave theory with a stably stratified shear flow. Their theory is concerned with an extension of classical first-order nonlinear wave theory correct to second order in wave amplitude and phase speed, and to first order in wavelength. These higher order corrections are neglected in the present comparison of the observations with theory. It is found (see Appendix II) that for a Boussinesq fluid with constant Brunt–Väisälä frequency, N_0, and constant wind shear, $u_0 = -kz$, the linear long-wave phase speed (c_0), a second-order correction to the first-order phase speed (c_1), and the parameter λ are

$$c_0 = \frac{kh}{\exp(s\pi/\mu) - 1}, \quad s = \pm 1, \pm 2, \cdots \tag{8}$$

$$c_1 = \frac{2ac_0\mu R \exp(s\pi/\mu)}{3h(\mu^2 + 9/4)}\left\{1 - (-1)^s \exp\left(\frac{-3s\pi}{2\mu}\right)\right\}, \tag{9}$$

$$\lambda = \left\{\frac{3h^3(\mu^2 + 9/4)(\exp(s\pi/\mu) + 1)}{2a\mu R(\mu^2 + 1)[\exp(s\pi/\mu - 1]^2 \times [1 - (-1)^s \exp(-3s\pi/2\mu)]}\right\}^{1/2}, \tag{10}$$

where

$$\mu = (\mathrm{Ri} - 1/4)^{1/2} = (N_0^2/k^2 - 1/4)^{1/2}$$

$$R = (1 + kz_m/c_0)^{1/2}[1 + 1/(4\mu^2)]^{1/2}(-1)^{(s-|s|)/2}$$

$$1 + kz_m/c_0 \doteq \exp[(\tan^{-1}2\mu)/\mu + (s - |s|)\pi/(2\mu)].$$

These expressions agree with those obtained by Maslowe and Redekopp (1980). Notice that the wavelength of the sech^2 wave is $2\pi\lambda$ (e.g., see p. 36 of Bhatnagar, 1979). Equation (8) indicates that for a positive mode number s, $c_0/kh > 0$, and the wave propagates in a direction opposite to the basic flow. For a negative mode number s, $c_0/kh > -1$, and the wave propagates in the same direction as the basic flow. The sign of the amplitude a in Eqs. (9) and (10) is dependent upon the sign of s. Thus, the solitary wave is a wave of elevation for positive s, while it is a wave of depression for negative s. We are particularly interested in the case of a solitary wave of depression for the lowest mode, $s = -1$, which has the highest phase speed and propagates in the same direction as the midtropospheric flow. The depth of the fluid is observed to be 9000 m (~300 mb) at the height where the disturbance is small (Fig. 8). The values of Brunt–Väisälä frequency, wind speed, shear, phase speed and wavelength for DAY and PIT are shown in Table 3.

The calculated linear phase speeds c_0, 65 and 61 m s^{-1} for DAY and PIT, respectively, are in reasonable agreement with the observed values of 55 m s^{-1}. The first-order corrections due to nonlinearity for the phase

TABLE 3. Parameters for estimating the phase speeds and wavelengths from DAY and PIT.

	h (m)	k (10^{-3} s^{-1})	s	Ri	μ	a (m)	c_0 (m s^{-1})	c_1 (m s^{-1})	λ (km)	L ($2\pi\lambda$)
DAY	9000	−5.74	−1	4.30	2.01	500	65	1.22	18.8	118
PIT	9000	−5.25	−1	4.97	2.17	500	61	0.36	19.7	124

speeds (c_1) are small compared with the first-order phase speeds (c_0). The phase speed is relatively insensitive to the degree of nonlinearity as pointed out by Noonan and Smith (1985). The wave amplitudes are more difficult to determine and are roughly estimated to be 500 m from the data in Fig. 8. The calculated wavelengths are about 35% less than observed values (about 185 km). Discrepancies between calculated and observed values may be due to model neglect of the detailed structure such as the weak stratification in the layer above the midtropospheric inversion and the assumption of a rigid top at the tropopause.

6. Concluding remarks

A mesoscale wave observed in numerous barograph traces from stations in the eastern United States on 6 March 1969, has an associated V-shaped pressure drop of 3 to 6 mb and is determined to be a solitary wave. The characteristics of this wave and its environment may be summarized as follows:

(i) the wave is in isolated quasi-steady form for a considerable time;
(ii) the wave appears to be an internal wave of depression;
(iii) there is strong convective activity near the origin of the wave;
(iv) there exists a midlevel inversion below a weakly stratified layer and above a stable layer;
(v) the midtropospheric inversion provides a base for the solitary wave to form and to travel horizontally;
(vi) the wave propagates in the direction of mid- and upper-tropospheric flow.

The wave is attributed to the perturbation of a midtropospheric inversion by a squall line. The generation mechanism for a mesoscale internal wave of depression or elevation is investigated by a simple model. The initial disturbance is everywhere a wave of depression or elevation depending upon the nondimensional number M which is related to the heating location and the structure of the atmosphere. In the present case, the available evidence indicates that an initial disturbance caused by latent heat production near a midtropospheric inversion has led to the formation of a single solitary wave of depression. The solitary wave propagates in a different direction from the squall line motion after it forms, and expands as an arc of about 40° with the center located at the point source. The solitary wave only propagates in the favorable direction of the mid- and upper tropospheric flow which explains why the solitary wave is only detected in this northeast oriented arc area. The characteristics of the wave appear to belong to the class of classical KdV solitary wave. The recent study of Uccellini and Koch (1987) suggests that the geostrophic imbalance associated with an upper-level jet streak may be a possible source of the mesoscale gravity waves with wavelength on the order of 100 km. However, it is not clear that this mechanism applies to the present case as the formation mechanism for isolated solitary waves differs from that of gravity wave packets. The weakly stratified layer in the upper troposphere is important in supporting the internal solitary-wave motion since the radiation damping of the wave energy is small. However, the eventual dissipation of the solitary wave downstream is partly due to this damping effect.

It has been shown that the effects of nonlinearity and dispersion in this case are the same order of magnitude. Thus, the wave may be classified as a mesoscale solitary wave. The phase speed and wavelength are determined by utilizing the theory of Gear and Grimshaw (1983). The theoretical description corresponding to the lowest eigenvalue mode describes the basic character of the solitary wave as a wave of depression with a preferred propagation in the direction of the basic flow. Both characteristics are verified by observation. The phase speeds calculated from Dayton, Ohio (DAY) and Pittsburgh, Pennsylvania (PIT) data are in agreement with the observed values. The wavelengths are somewhat less than the observed values. Discrepancies between calculated and observed values may be due to model neglect of the detailed structure of the atmosphere such as the weak stratification in the layer above the midtropospheric inversion and the assumption of a rigid top at the tropopause.

Acknowledgments. The authors wish to express their gratitude to Dr. C. W. Kreitzberg of Drexel University for his encouragement on this work and the review of the manuscript. The discussion with Dr. R. B. Smith of Yale University was very helpful. Valuable comments from Drs. S. E. Koch and M. J. Pecnick of NASA/GSFC are appreciated. Comments from anonymous reviewers greatly improved the quality of the manuscript. This work was partially supported by the NSF under Grant ATM-8311593. We thank the mesoscale group of the Drexel University for helping the computational work.

APPENDIX A

Asymptotic Solution of Equation (5)

The derivation of the asymptotic form of Eq. (5) follows closely the method of stationary phase described in Miles (1971). The first integral is expressed as

$$I = \int_{-\infty}^{\infty} A(\omega) \exp(i\phi(\omega))d\omega \tag{A1}$$

$$\phi(\omega) = Nz_1|k|/\omega + \omega t \tag{A2}$$

$$A(\omega) = 1/\{\omega(\omega^2 - iNH\omega|k| - g'Hk^2)\}. \tag{A3}$$

The approximate solution of (A1) for large t is

$$I = (2\pi/|\phi_s''|)^{1/2} A_s \exp[i(\phi_s + (\pi/4)\,\mathrm{sgn}\phi'')]. \tag{A4}$$

The point of stationary phase can be obtained by taking $\phi'(\omega) = 0$, which leads to $\omega_s = (Nz_1|k|/t)^{1/2}$. Substituting ω_s into (A3), and applying the method of stationary phase (A4) for large time, we obtain

$$I = \frac{\pi^{1/2}t^{3/4} \exp[i(2(Nz_1|k|t)^{1/2} + \pi/4)]}{(Nz_1)^{1/4}|k|^{5/4}[Nz_1 - i(N^3H^2z_1|k|t)^{1/2} - g'H|k|t]}. \tag{A5}$$

Substituting (A5) into Eq. (5) gives

$$\eta = \frac{igQ_0b(z+H)t^{3/4}}{4\pi^{1/2}c_p\bar{T}(Nz_1)^{1/4}} \times \int_{-\infty}^{\infty} \frac{k^{3/4}e^{-bk}}{[Nz_1 - i(N^3H^2z_1kt)^{1/2} - g'Hkt]} \times \{\exp[i(kx + 2(Nz_1kt)^{1/2} + \pi/4)] + \exp[i(-kx + 2(Nz_1kt)^{1/2} + \pi/4)]\}dk. \tag{A6}$$

The method of stationary phase is applied to (A6) again for large x. The second term has a point of stationary phase for $x > 0$, and the first term has a point of stationary phase for $x < 0$. Equation (6) is the solution.

APPENDIX B

Solitary Wave Theory of Gear and Grimshaw

The theory of Gear and Grimshaw (1983) assumes a separation of variables of the vertical displacement

$$\eta = \alpha A(x)\phi(z), \tag{B1}$$

where $f(z)$ is the modal function which satisfies the following eigenvalue problem:

$$[\rho_0(c_0 - u_0)^2\phi_z]_z + \rho_0N^2\phi = 0 \tag{B2}$$

$$\phi = 0 \quad \text{at} \quad z = 0 \quad \text{and} \quad z = h.$$

At the upper boundary it is assumed that there is no vertical motion. This condition is roughly satisfied since the vertical motion is very weak near the tropopause (Fig. 8). In the present case we assume h to be the depth of the tropopause as mentioned above. A vertically propagating wave will be partially reflected back toward the earth if the change in stability across the tropopause is abrupt. The solitary wave solution is

$$A(X) = a\,\mathrm{sech}^2(X/\lambda). \tag{B3}$$

Definitions of symbols can be found in Gear and Grimshaw. For a Boussinesq fluid with constant Brunt–Väisälä frequency, N_0, and constant wind shear, $u_0 = -kz$, the phase speeds and wavelength are derived by Gear and Grimshaw and expressed in Eqs. (8)–(10). Notice that the wavelength of the sech^2 wave is $2\pi\lambda$ (e.g., see p. 36 of Bhatnagar, 1979).

REFERENCES

Abdullah, A. J., 1955: The atmospheric solitary wave. *Bull. Amer. Meteor. Soc.*, **10**, 511–518.

Benjamin, T. B., 1966: Internal waves of finite amplitude and permanent form. *J. Fluid Mech.*, **25**, 241–270.

——, 1967: Internal waves of permanent form in fluids of great depth. *J. Fluid Mech.*, **25**, 559–592.

Bhatnagar, P. L., 1979: *Nonlinear Waves in One-dimensional Dispersive Systems*. Clarendon Press, 142 pp.

Bosart, L. F., and J. P. Cussen, 1973: Gravity wave phenomena accompanying east coast cyclogenesis. *Mon. Wea. Rev.*, **101**, 446–454.

——, and F. Sanders, 1986: Mesoscale structure in the Megalopolitan Snowstorm of 11–12 February 1983. Part III: A large-amplitude gravity wave. *J. Atmos. Sci.*, **43**, 924–939.

Brunk, I. W., 1949: The pressure pulsation of 11 April 1944. *J. Meteor.*, **6**, 181–187.

Christie, D. R., K. J. Muirhead and A. L. Hales, 1978: On solitary waves in the atmosphere. *J. Atmos. Sci.*, **35**, 805–825.

——, —— and ——, 1979: Intrusive density flows in the lower troposphere: A source of atmospheric solitons. *J. Geophys. Res.*, **84**, 4959–4970.

——, —— and R. H. Clarke, 1981: Solitary waves in the lower atmosphere. *Nature*, **293**, 46–49.

Crook, N. A., 1986: The effect of ambient stratification and moisture on the motion of atmospheric undular bores. *J. Atmos. Sci.*, **43**, 171–181.

Curry, M. J., and R. C. Murty, 1974: Thunderstorm-generated gravity waves. *J. Atmos. Sci.*, **31**, 1402–1408.

Davis, R. E., and A. Acrivos, 1967: Solitary internal waves in deep water. *J. Fluid Mech.*, **29**, 593–607.

Doviak, R. J., and R. Ge, 1984: An atmospheric solitary gust observed with a Doppler radar, a tall tower and a surface network. *J. Atmos. Sci.*, **41**, 2559–2573.

Eom, J. K., 1975: Analysis of the internal gravity wave occurrence of 19 April 1970 in the Midwest. *Mon. Wea. Rev.*, **103**, 217–226.

Erickson, C. O., and L. E. Whitney, Jr., 1973: Picture of the month: Gravity waves following severe thunderstorms. *Mon. Wea. Rev.*, **101**, 708–711.

Ferguson, H. L., 1967: Mathematical and synoptic aspects of a small scale wave disturbance over the Lower Great Lakes. *J. Appl. Meteor.*, **6**, 523–529.

Geisler, J. E., and F. P. Bretherton, 1969: The sea-breeze forerunner. *J. Atmos. Sci.*, **26**, 82–95.

Gear, J. A., and R. Grimshaw, 1983: A second-order theory for solitary waves in shallow fluid. *Phys. Fluid*, **26**, 14–29.

Grimshaw, R., 1980/81: Solitary waves in a compressible fluid. *Pure Appl. Geophys.*, **119**, 780–797.

——, 1981a: Evolution equations for long nonlinear internal waves in stratified shear flows. *Stud. Appl. Math.*, **65**, 159–188.

——, 1981b: A second order theory for solitary waves in deep fluids. *Phys. Fluids,* **24,** 1611–1618.

Haltiner, G. J., and R. T. Williams, 1980: *Numerical Prediction and Dynamic Meteorology.* Wiley and Sons, 477 pp.

Hasse, S. P., and R. K. Smith, 1984: Morning glory wave clouds in Oklahoma: A case study. *Mon. Wea. Rev.,* **112,** 2078–2089.

Joseph, R. I., 1977: Solitary waves in a finite depth fluid. *J. Phys. A., Math. Nucl. Gen.,* **10,** L225–227.

Koop, C. G., and G. Butler, 1981: An investigation of internal solitary waves in a two-fluid system. *J. Fluid Mech.,* **112,** 225–251.

Lin, Y.-L., and R. B. Smith, 1986: Transient dynamics of airflow near a local heat source. *J. Atmos. Sci.,* **43,** 40–49.

Lindzen, R. S., and K.-K. Tung, 1976: Banded convective activity and ducted gravity waves. *Mon. Wea. Rev.,* **104,** 1602–1617.

Long, R. L., 1965: On the Boussinesq approximation and its role in the theory of internal waves. *Tellus,* **17,** 46–52.

Maslowe, S. A., and L. G. Redekopp, 1980: Long nonlinear waves in stratified shear flows. *J. Fluid Mech.,* **101,** 321–348.

Miles, J. W., 1971: *Integral Transforms in Applied Mathematics.* Cambridge University Press, 97 pp.

——, 1979: On internal solitary waves. *Tellus,* **31,** 456–462.

Miller, D. A., and F. Sanders, 1980: Mesoscale conditions for the severe convection of 3 April 1974 in the east-central United States. *J. Atmos. Sci.,* **37,** 1041–1055.

Noonan, J. A., and R. K. Smith, 1985: Linear and weakly nonlinear internal wave theories applied to "Morning Glory" waves. *Geophys. Astrophys. Fluid Dyn.,* **33,** 123–143.

Ono, H., 1975: Algebraic solitary waves in stratified fluids. *J. Phys. Soc. Japan,* **39,** 1082–1091.

Peters, A. S., and J. J. Stoker, 1960: Solitary waves in liquids having non-constant density. *Commun. Pure Appl. Math.,* **13,** 115–164.

Pecnick, M. J., and J. A. Young, 1984: Mechanics of a strong subsynoptic gravity wave deduced from satellite and surface observations. *J. Atmos. Sci.,* **41,** 1850–1862.

Raymond, D. J., 1983: Wave-CISK in mass flux form. *J. Atmos. Sci.,* **40,** 2561–2572.

Smith, R. B., and Y.-L. Lin, 1982: The addition of heat to a stratified airstream with application to the dynamics of orographic rain. *Quart. J. Roy. Meteor. Soc.,* **108,** 353–378.

Stobie, J. G., F. Einaudi and L. W. Uccellini, 1983: A case study of gravity waves-convective storms interaction: 9 May 1979. *J. Atmos. Sci.,* **40,** 2804–2830.

Uccellini, L. W., 1975: A case study of apparent gravity wave initiation of severe convective storms. *Mon. Wea. Rev.,* **103,** 497–513.

——, and S. E. Koch, 1987: The synoptic setting and possible energy sources for mesoscale wave disturbances. *Mon. Wea. Rev.,* **115,** 721–729.

Wagner, J. A., 1962: Gravity wave over New England, 12 April 1961. *Mon. Wea. Rev.,* **90,** 431–436.